

## The phase transition behaviour of linear polyethylenes at high pressure

G.W.H. Höhne<sup>a,\*</sup>, J.E.K. Schawe<sup>a</sup>, A.I. Shulgin<sup>b</sup>

<sup>a</sup> Universität Ulm, Sektion für Kalorimetrie, D-089069 Ulm, Germany

<sup>b</sup> Karpov Institute of Physical Chemistry, Ul. Obukha 10, 103064 Moscow, Russia

Received 12 November 1996; received in revised form 21 January 1997; accepted 26 January 1997

### Abstract

The influence of the pressure on the melting behaviour of different linear polyethylene samples with molar masses from 5 to 4000 kg mol<sup>-1</sup> has been investigated by three methods: crystallization and melting at different pressure in the high pressure DSC, crystallization at different pressure and subsequent melting at normal pressure, crystallization at high pressure (500 MPa) and melting at normal pressure but at different heating rates. The dependence of melting temperature and enthalpy change on crystallization pressure are given. The high pressure crystallized material seems to be in a metastable state (after decompression) with larger enthalpy and higher melting temperature than in the equilibrium state. The high molar mass sample behaves like a single component system, whereas that with low molar mass shows a complex multicomponent phase separation behaviour. © 1997 Elsevier Science B.V.

**Keywords:** Differential scanning calorimetry; DSC; Enthalpy; High pressure; Melting; Phase diagram; Polyethylene

### 1. Introduction

Polyethylene (PE) has long been used as a model substance in the study of the melting behaviour of semi-crystalline polymers. This is because PE is made up of very simple chain molecules. The intermolecular chemical and physical interaction energies are very weak and all conformation energies are well known. In addition, the oligomers, *n*-alkanes and cyclic alkanes, are available within a wide range of monomer numbers *n* and their crystallization behaviour and structure are well known. Based on a large body of experimental results there have been several descriptions of the melting behaviour of PE

[1–8] and it is probable that the crystallization behaviour of at least this polymer is well understood. However, most of the experimental results have been obtained at normal pressure and the resulting theoretical approaches are only valid at that pressure. There are not enough high pressure experiments [9–13] to extend the models into this region with any confidence.

This paper presents DSC results on the melting behaviour of pressure crystallized PE at high pressures (up to 550 MPa) and, using conventional DSC, at atmospheric pressure.

Together with data for the high pressure behaviour of pure *n*-alkanes and *n*-alkane mixtures already published [14], these results will probe the validity of the several theoretical models in the high pressure region. The detailed discussion of our results would, however,

\*Corresponding author. Fax: 0049-731-5023112.

greatly extend this paper and this will be done elsewhere.

## 2. Experimental

### 2.1. Apparatus

All measurements were made in power compensated differential scanning calorimeters (DSC). In the case of normal pressure measurements we used a Perkin Elmer DSC 7 with careful control of the block temperature. The other measurements were performed in a home-made power compensated high-pressure DSC (HP-DSC) [15], suitable for the pressure region from ambient to 550 MPa with silicon oil as pressure medium.

Samples (mass: 1 to 10 mg) were always hermetically sealed in aluminium crucibles to exclude contact with the pressure medium (silicone oil). They were heated and cooled at the relevant pressure at rates from 1 to 20 K/min. Calibration was done as usual [16–18]. In addition one small indium sample was always put in the reference cell for ‘online’ calibration control. The check whether, and how much, a sample and reference cell behaves differently has been done separately at different pressures.

### 2.2. Samples

The following types of linear polyethylene were used:

GUR ( $M_w = 4000 \text{ kg mol}^{-1}$ ,  $M_w/M_n = 6.5(106)$ ; 13.5 (412), HOECHST AG)

HDPE (Lupolen 6011,  $M_w = 63 \text{ kg mol}^{-1}$ ,  $M_w/M_n = 2$ , SCB < 1 per 1000 C-atoms, BASF); (PEL 3,  $M_w = 350 \text{ kg mol}^{-1}$ ,  $M_w/M_n = 2$ , SCB < 0.5 per 1000 C, Russia)

PE-WAX (PE 130,  $M_w = 4.6 \text{ kg mol}^{-1}$ ,  $M_w/M_n = 3.6$ , HOECHST AG)

The material in question was either bulk crystallized in a high pressure dilatometer [19] by slow cooling ( $0.5 \text{ K min}^{-1}$ ) at the respective pressure, released to normal pressure and then cut into suitable pieces (2 to 10 mg), or cut as received from the manufacturer and both melted and crystallized in the high pressure DSC.

## 3. Results

The influence of pressure on the melting behaviour of the different PE samples was investigated in three ways:

1. Crystallization and melting at different pressure in the HP-DSC
2. Crystallization at different pressure and subsequent melting at normal pressure
3. Crystallization at high pressure (500 MPa) and melting at normal pressure but with different heating rates.

### 3.1. HP-DSC measurements

Samples (mass: 5 to 10 mg) were heated in the HP-DSC at the appropriate pressure to temperatures 20 K above the melting temperature, cooled at a rate of  $10 \text{ K min}^{-1}$  and reheated at  $10 \text{ K min}^{-1}$ . From the melting curve the peak maximum temperature was determined and corrected relative to the measured melting temperature of an indium sample which was always in the reference cell. The pressure dependence of the fusion temperature and enthalpy of indium is well known [19], and we used it for calibration. The results for three different PE materials are shown in Figs. 1–3.

The symbols reproduce the corrected peak temperatures and the solid lines present the respective regression curves. The dashed line shows the pressure dependence of the fusion temperature of an extended chain *n*-alkane crystal with an infinite number of  $\text{CH}_2$ -groups. This function was derived from the pressure dependence of the fusion temperature of different *n*-alkanes [14]:

$$T_{\text{fus}}^{\infty}(p) = 414.8 + 0.2503p - 1.348 \times 10^{-4}p^2 \quad (1)$$

(*T*: temperature in K, *p*: pressure in MPa)

It is used to compare the melting behaviour of the real PE samples with that of an ideal crystal. In reality the melting peak of PE (Fig. 4) is broader than that of pure substances so that there is a melting range rather than a specific melting temperature. Nevertheless the peak maximum characterizes the maximum melt temperature of the sample to a good approximation. The exact connection between the measured peak max-

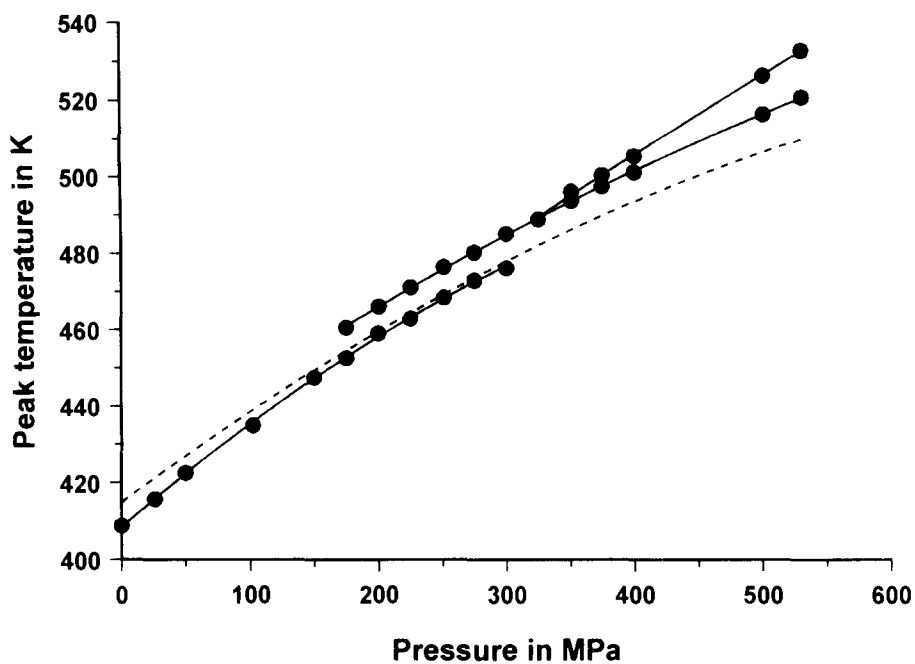


Fig. 1. Peak maximum temperatures of GUR 106, measured at different pressure in the HP-DSC after crystallization at the same pressure (mass: ca. 7 mg, heating rate:  $10 \text{ K min}^{-1}$ ). Solid line: regression curve, dashed line: melting temperature of an infinite alkane crystal (Eq. (1)).

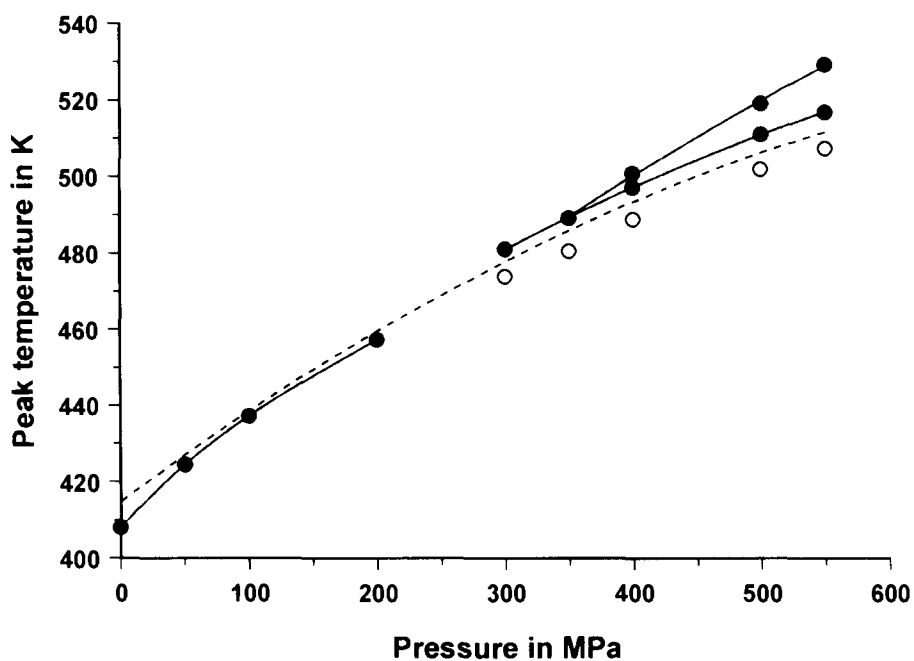


Fig. 2. Peak maximum temperatures of HDPE 6011, measured at different pressures in the HP-DSC after crystallization at the same pressure (mass: ca. 7 mg, heating rate:  $10 \text{ K min}^{-1}$ ). Solid line: regression curve, dashed line: melting temperature of an infinite alkane crystal (Eq. (1)), open circles: additional pre-peak.

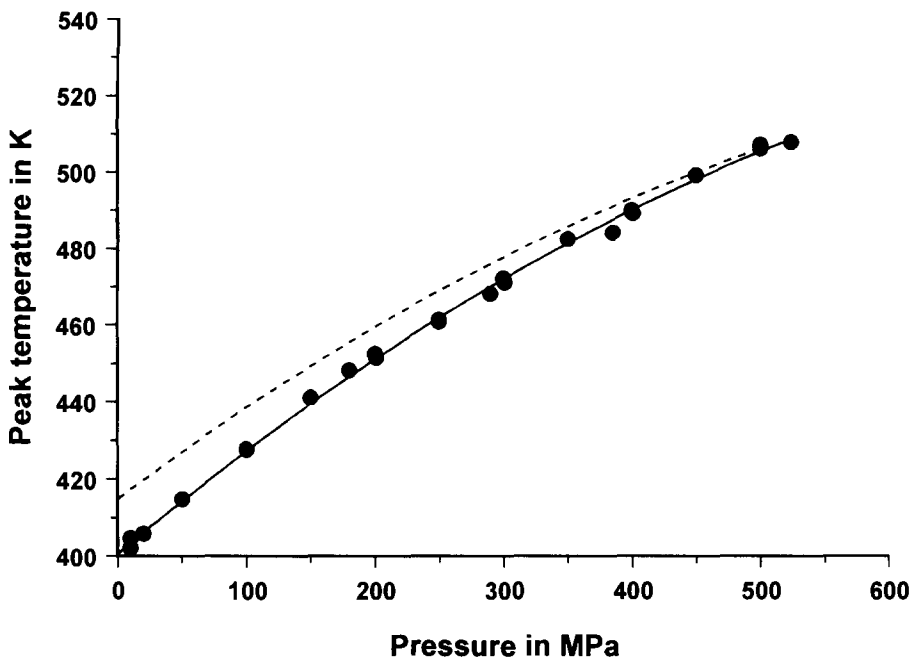


Fig. 3. Peak maximum temperatures of PE 130, measured at different pressures in the HP-DSC after crystallization at the same pressure (mass: ca. 7 mg, heating rate:  $10 \text{ K min}^{-1}$ ). Solid line: regression curve, dashed line: melting temperature of an infinite alkane crystal (Eq. (1)).

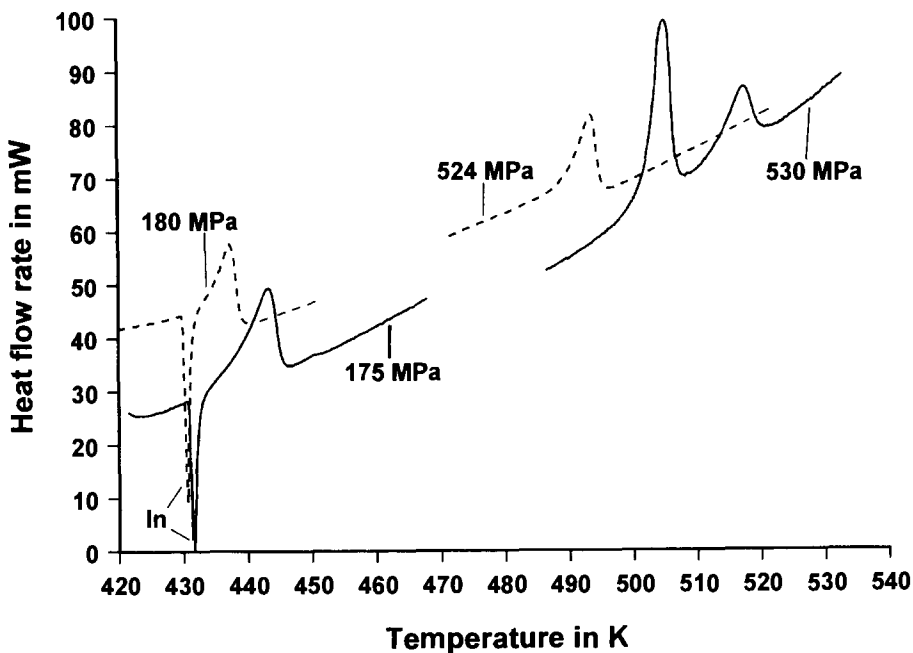


Fig. 4. Examples of the HP-DSC melting curves of PE 130 (dashed curves) and GUR 106 (solid curves) at different pressure. (Masses: ca. 7 mg, heating rate:  $10 \text{ K min}^{-1}$ ). The additional melting peak of indium points into the wrong direction, because the calibration sample is placed in the reference crucible).

imum temperature and the real maximum melting temperature of the sample is not easy to determine. For a dynamic calorimeter, such as the DSC, the correction depends on sample mass and heating rate including heat transfer and kinetic conditions. However, for a given sample and constant heating rate this correction is constant and does not depend on pressure, so that the real maximum melting temperature curve is almost parallel to the measured regression line.

Keeping this in mind, Figs. 1 and 2 show that GUR and HDPE melt as long-chain *n*-alkanes because the measured curves (solid lines) are, at least above 130 MPa, parallel to that from the ideal crystal (dashed line), whereas the behaviour of PE 130 (Fig. 3) is very different.

There are other striking differences between these samples: for both GUR and HDPE the low pressure and the high pressure regression lines do not merge (if we disregard the small (ca. 7%) pre-peak of HDPE 6011 (Fig. 2) which may be related to low molar mass components). In the pressure region from 180 to 300 MPa there were two well-separated peaks, the first decreasing and the second increasing with pressure (Fig. 1) and a continuously changing area ratio. There is no continuous increase in the temperature of a single melting peak as for PE 130 (Fig. 3). It is well known that PE forms lamellae of folded-chain crystals (FCC) at lower pressure – with a melting temperature comparable to that of *n*-alkanes ( $n = 300$ ) with the same length (38 nm) – whereas it forms extended chain crystals (ECC) at higher pressure and they melt at temperatures where the infinite *n*-alkane melts (Eq. (1)). The difference between these two melting points is 9 K at normal pressure and this corresponds exactly to the gap between the two regression lines in Figs. 1 and 2.

From the GUR results (Fig. 1) it is clear, that the change from FCC to ECC, is discontinuous. Between 180 and 300 MPa both types of crystals coexist. For PE 130 (Fig. 3) there is no high molecular mass ECC melting peak at all, the measured melting temperatures are too low, even at the highest pressure. Furthermore, the well known (hexagonal) high pressure conformationally disordered phase (CONDIS [20]) of PE does not occur with PE 130, whereas it is found for the other two samples. An interesting fact is that the melting peak of the CONDIS phase is broader than

that of the low pressure phase (cf. Fig. 4). Obviously this transition is more lambda-shaped and thus not a common first-order transition; it must at least contain components of an ‘order–disorder’ transition.

A small additional peak is visible in the melting curves of HDPE and PE 130 at pressures above 300 MPa (Figs. 2 and 3, open circles). This seems to indicate some phase separation within the rather complex mixture of low molecular weight components at high pressure. A similar effect has been found for *n*-alkane mixtures [14]. It is also possible that a small amount of a less common triclinic phase has been formed in this pressure region, which is metastable and melts about 9 K lower than the stable orthorhombic phase [21].

### 3.2. DSC measurements of high-pressure crystallized PE

Samples (mass: 20 g) of GUR were cooled slowly ( $0.5 \text{ K min}^{-1}$ ) from the melt at different pressures in a high-pressure dilatometer. After decompression small samples (mass: 4 to 8 mg) were cut from the bulk, encapsulated and measured in the DSC at normal pressure with a heating rate of  $10 \text{ K min}^{-1}$  (purge gas: nitrogen,  $20 \text{ ml min}^{-1}$ ). From the zeroline-corrected curve, both the peak maximum temperature and the specific heat of fusion were determined as usual [22].

Figs. 5 and 6 show the results for two different GUR products. GUR 412, which we used first, unfortunately turned out to be, perhaps, bimodal distributed in molar mass, so we changed to another product: GUR 106 which is monomodal distributed. There is in general no big difference between the results for these two samples. For both, the same pressure dependence of the specific heat of fusion is found (Fig. 6). The behaviour may be explained by two effects: first the well known increase of the degree of crystallinity with pressure and, second, a slight dependence of the total melting enthalpy on the crystallization pressure with a maximum at ca. 400 MPa. The same result is found for the temperature of the main melting peak, which increases from  $140^\circ\text{C}$  ( $p_{\text{cryst}} = 180 \text{ MPa}$ ) to  $148^\circ\text{C}$  ( $p_{\text{cryst}} = 400 \text{ MPa}$ ) decreasing again to  $146.5^\circ\text{C}$  for higher crystallization pressures. This result corresponds to density measurements on the same samples which also show a slight maximum for samples crys-

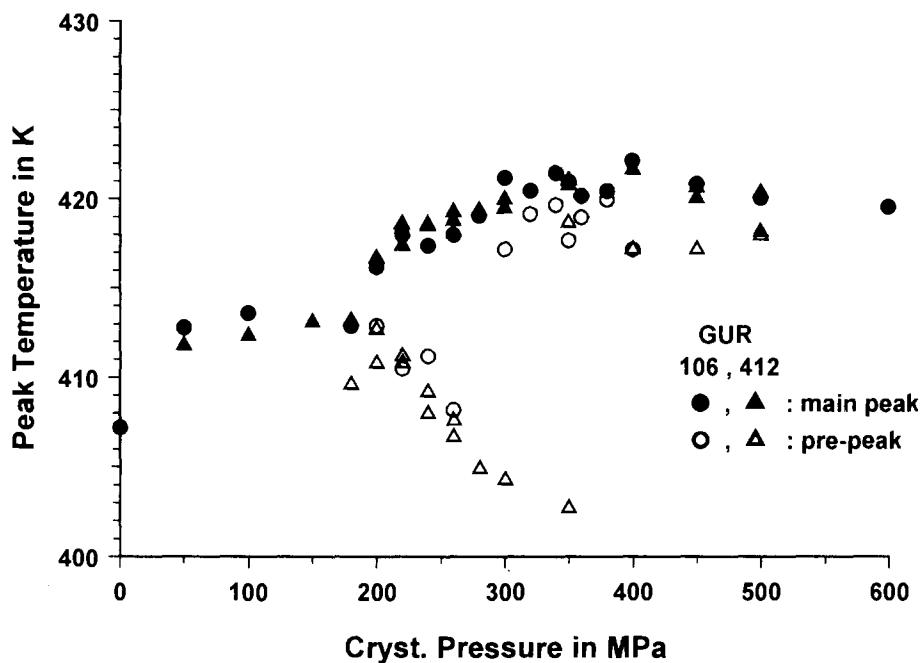


Fig. 5. Peak maximum temperatures of two different types of GUR measured at ambient pressure in a conventional DSC of samples crystallized at the given pressure in a high pressure dilatometer. Solid symbols: main peak, open symbols: pre-peak. (Masses: ca. 7 mg, heating rate:  $10 \text{ K min}^{-1}$ ).

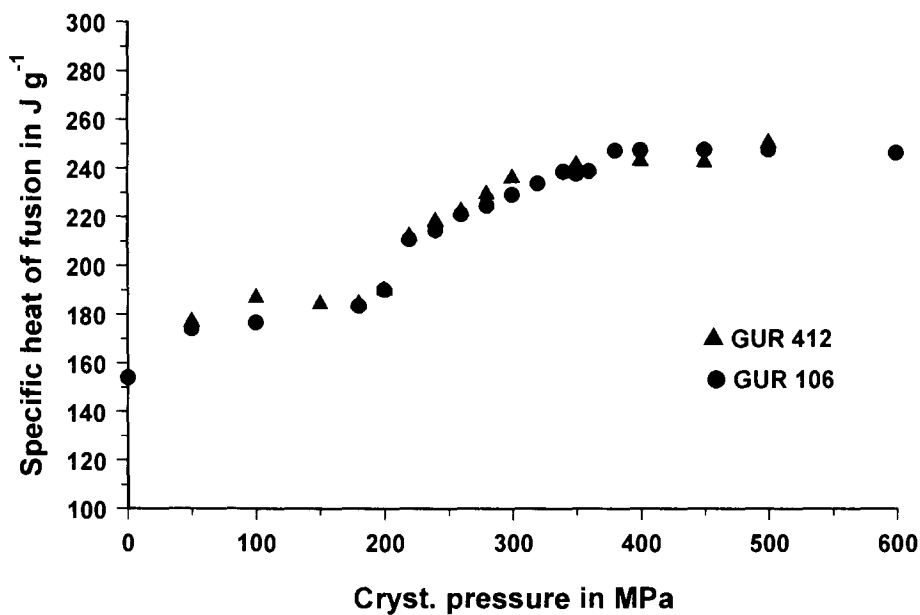


Fig. 6. Total specific heat of fusion of two different types of GUR measured at ambient pressure in a conventional DSC of samples crystallized at the given pressure in a high pressure dilatometer. (Masses: ca. 7 mg, heating rate:  $10 \text{ K min}^{-1}$ ).

tallized at 350 MPa [23]. The enthalpy of fusion of *n*-alkanes has a similar maximum at pressures of ca. 300 MPa [14], obviously the decompressed samples 'remember' the crystallization pressure.

Differences between both GUR samples exist relative to the second (small) peak on the left shoulder of the main peak, which for GUR 412 is visible in a broader region of the crystallization pressure than is the case for GUR 106. Obviously there is some phase separation visible, probably from lower molecular weight components.

The decrease of the respective melting temperature with crystallization temperature can be explained by a decrease of crystallite size and/or an increase of their surface energy.

Comparing the melting behaviour at ambient pressure (Fig. 5) with that at crystallization pressure (Fig. 1) the question arises, why in the pressure region from 180 to 300 MPa the melting temperature increases continuously in the case of ambient pressure measurements, whereas it 'jumps' to the respective value of the ECC phase (both being parallel to the curve of a fixed (infinite) lamella thickness melting temperature versus pressure function) for melting at the crystallization pressure. At ambient pressure the melting temperature increases with crystallization pressure, if the same would be the case for high pressure melting, the measured temperature–pressure function could not, however, be parallel to the respective curve of an ideal infinite alkane crystal. Obviously the solid state cannot be the same; there must be some significant change of the structure on pressure release. To characterize these differences, X-ray studies are needed at both high and ambient pressures.

To obtain additional information we investigated the melting behaviour of high pressure (500 MPa) crystallized samples at different heating rates in the DSC at ambient pressure.

Again the peak maximum temperature was evaluated. From theoretical considerations on heat transfer in dynamical calorimeters it follows that the peak maximum is shifted to higher temperatures with the squareroot of mass as well as the squareroot of the heating rate [24]. To eliminate that influence and get the true melting temperature we have to plot the measured peak maximum temperature against the squareroot of the product of sample mass and heating rate and extrapolate to an abscissa of zero. Fig. 7 gives

the results after different treatments. There are two sets of straight lines with different slopes and different intersections with the ordinate axis. All samples crystallized at high pressure have an intersection point of 412 to 414 K in good agreement with literature values of ECC–PE [2] or the value for an infinite *n*-alkane ([2,14] and Eq. (1)). However, the slopes of the regression lines are different. Annealed high molar mass samples (GUR 106, PEL 3) definitely have larger slopes than that for low molar mass PE 6011. Comparing these slopes with those of the samples crystallized at ambient pressure (Fig. 7, lower part) we find that the small slopes are the same in both cases and also agree with that of the melting peak for alkanes at ambient pressure [25]. We must conclude that the small slope reflects the influence of the heat transfer conditions, whereas the larger slope points to additional effects leading to a delay in melting. The reason for this may be kinetically hindered melting (overheating) as Wunderlich has suggested [2] or an increased melting temperature because of an increased enthalpy and/or decreased entropy of fusion for the high pressure crystallized samples. The latter supposition is supported by the observation, that annealing of the high pressure crystallized GUR 106 sample at a temperature 1.5 K below the melting temperature decreases the slope of the respective melting peaks to the normal value (see Fig. 7). Obviously the annealing procedure destroys the special structure of the decompressed solid PE samples. This can be understood if we assume a metastable high densified state within the solid sample after decompression, which is connected with a higher enthalpy because of a lower distance between the chains, whereas the melt is in the non-densified state with normal enthalpy. The relaxation of the metastable state to the equilibrium state at normal pressure needs time, which in turn depends on temperature.

This way the steeper slope of the high pressure crystallized samples may be explained by (i) a higher melting temperature because of a higher enthalpy (and almost unchanged entropy) together with (ii) a relaxation process from metastable to stable state which decreases the enthalpy and melting temperature but needs time and thus is of less influence at higher heating rates than at lower ones.

Another series of experiments was made with two samples of high pressure (500 MPa) crystallized PE

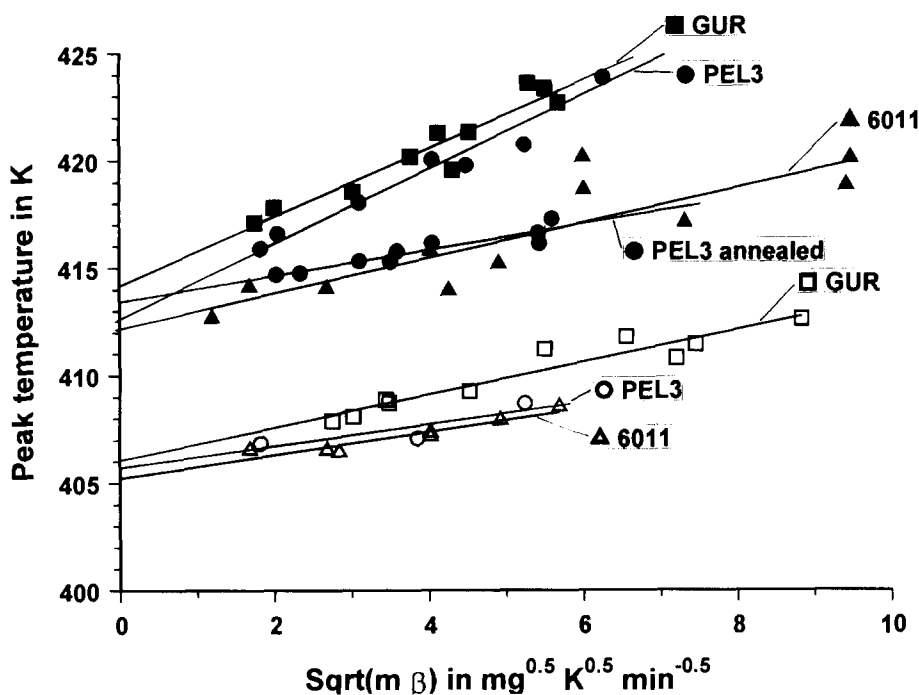


Fig. 7. Peak maximum temperatures of several samples (masses: 1 to 10 mg) of different types of PE measured at ambient pressure in a conventional DSC at different heating rates (1 to 20 K min<sup>-1</sup>). The abscissa is the square-root of the product of mass times heating rate. Solid symbols: Samples crystallized at 500 MPa in a high pressure dilatometer, open symbols: samples crystallized at ambient pressure.

(GUR 106 and PE 130) by heating them (5 K min<sup>-1</sup>) in the DSC at ambient pressure up to different temperatures within the melting region, rapidly cooling (80 K min<sup>-1</sup>) and reheating (5 K min<sup>-1</sup>) up to the melt. As a result GUR transforms successively from the ECC to FCC state proportional to the amount of the ECC which was molten at the reversal point of the temperature during the first run (Fig. 8). Accordingly, the upper peak decreases and the lower one increases without any additional shift on the temperature scale as the changed mass fractions would cause. The distance of both peaks is somewhat larger than 9 K in accordance with Fig. 7. In contrast to this result Fig. 9 looks quite different. Stopping the first run within the main melting peak now gives a 'valley' at the reversal point. Again the peak of the material molten during the first run is shifted to lower temperature but not at a constant value. A well-separated small peak is found on the high temperature side but below the ECC melting temperature of GUR. This small peak is not found if we melt the sample at crystallization pressure in the HP-DSC. Obviously

there must be some phase separation process during decompression of the wax sample. As the transition from ECC to FCC crystals does not occur in this sample, the peak separation must be otherwise explained. We believe that the origin lies in a complicated pressure-dependent phase diagram of a multi-component mixture. The composition of the solid phase is different for samples crystallized at high pressure from that obtained at normal pressure. The metastable state at normal pressure is 'frozen' on decompression and transforms to the stable one on first melting. The decreased melting temperature may be explained by a 'Porter parameter' that is lower at ambient pressure and which controls the phase behaviour as in binary *n*-alkane mixtures [14].

#### 4. Conclusions

The different results may be combined as follows:

The high pressure melting behaviour of various pressure-crystallized polyethylenes is different



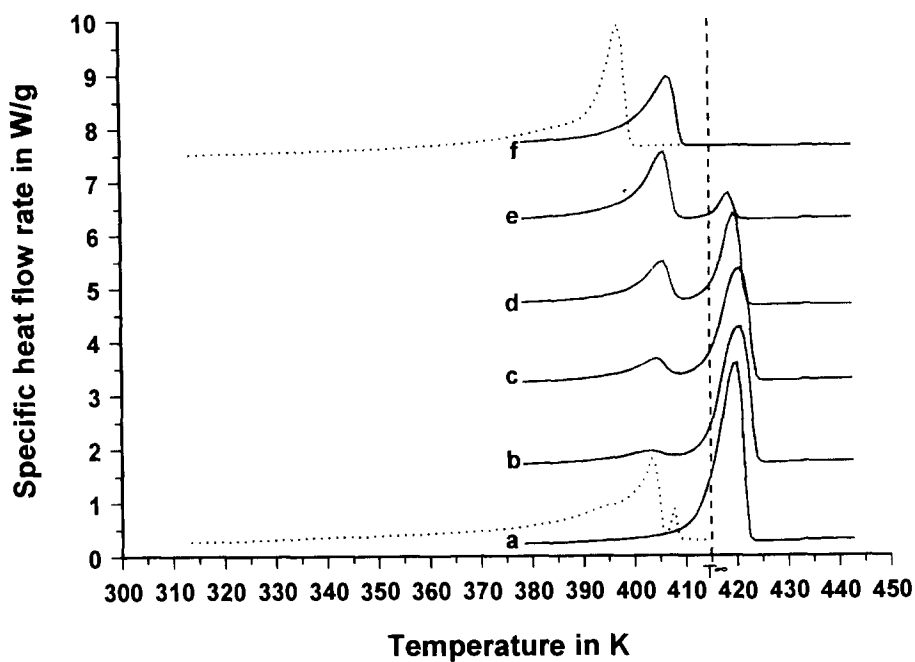


Fig. 8. Melting curves of GUR 106 (crystallized at 500 MPa in a high pressure dilatometer) measured in a conventional DSC at ambient pressure (masses: ca. 5 mg, heating rate:  $5 \text{ K min}^{-1}$ ) but with a different history: (a) 1st run, and reruns after stop (and immediately fast cooling) of the 1st run at (b) 418 K, (c) 420 K, (d) 422 K, (e) 423 K, and (f) 425 K. (Dotted curves similar results from PE-Wax (see Fig. 9) for comparison).

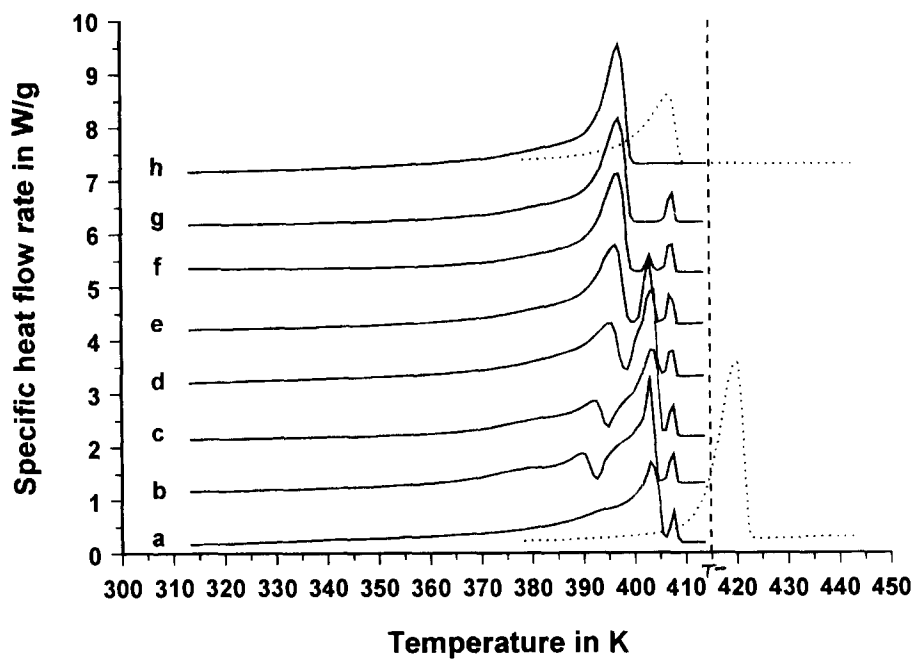


Fig. 9. Melting curves of PE 130 (crystallized at 500 MPa in a high pressure dilatometer) measured in a conventional DSC at ambient pressure (masses: ca. 5 mg, heating rate:  $5 \text{ K min}^{-1}$ ) but with different history: (a) 1st run, and reruns after stop (and immediately fast cooling) of the 1st run at (b) 393 K, (c) 397 K, (d) 401 K, (e) 403 K, (f) 405 K, (g) 406 K and (h) 411 K. (Dotted curves similar results from GUR 106 (see Fig. 8) for comparison).

from that at ambient pressure after decompression. The structure of the high pressure solid differs from that of the decompressed sample which seems to be metastable at ambient conditions.

The metastable state (with higher enthalpy at ambient pressure) relaxes to the stable one. The relaxation time depends on temperature.

The very high molar mass sample (GUR) behaves like a single component system which exists in two different phases of FCC and ECC respectively.

The very low molecular mass sample (PE 130) behaves like a multi-component mixture similar to *n*-alkane mixtures. The demixing and phase separation behaviour depends on pressure and may be frozen by decompression.

There are a lot of questions which cannot yet be answered. Additional high-pressure investigations, DSC measurements and the use of other techniques such as X-rays are necessary to confirm our conclusions and come to a convincing picture of the phase behaviour of the different polyethylenes.

## References

- [1] P.J. Flory, *J. Chem. Phys.*, 17(3) (1949) 223–240.
- [2] B. Wunderlich and G. Czornyj, *Macromolecules*, 10 (1977) 906–913.
- [3] B. Holl, B. Heise and H.G. Kilian, *Colloid. Polym. Sci.*, 261 (1983) 978–992.
- [4] R.G. Alamo and L. Mandelkern, *Macromolecules*, 22 (1989) 1273–1277.
- [5] G. Kanig, *Colloid. Polym. Sci.*, 269 (1991) 1118–1125.
- [6] R.G. Alamo and L. Mandelkern, *Thermochim. Acta*, 238 (1994) 155–201.
- [7] R. Mutter, W. Stille and G. Strobl, report (1993).
- [8] A. Keller, M. Hikosaka, S. Rastogi, A. Toda, J.P. Barham and G. Goldbeck-Wood, *J. Mater. Sci.*, 29 (1994) 2579–2604.
- [9] B. Wunderlich and L. Melillo, *Makromol. Chem.*, 118 (1968) 250.
- [10] D.C. Basset and B.A. Khalifa, *Polymer*, 17 (1976) 275.
- [11] M. Yasuniwa, C. Nakafuku and T. Takemura, *Polym. J.*, 4(5) (1973) 526–533.
- [12] M. Hikosaka, S. Rastogi, A. Keller and H. Kawataba, *J. Macromol. Sci.*, B31(1) (1994) 87–131.
- [13] C. Nakafuku, *Polymer*, 27(9) (1995) 917–927.
- [14] G.W.H. Höhne and K. Blankenhorn, *Thermochim. Acta*, 238 (1994) 351–370.
- [15] K. Blankenhorn and G.W.H. Höhne, *Thermochim. Acta*, 187 (1991) 219–224.
- [16] G.W.H. Höhne, H.K. Cammenga, W. Eysel, E. Gmelin and W. Hemminger, *Thermochim. Acta*, 160 (1990) 1–12.
- [17] H.K. Cammenga, W. Eysel, E. Gmelin, W. Hemminger, G.W.H. Höhne and S.M. Sarge, *Thermochim. Acta*, 219 (1993) 333–342.
- [18] S.M. Sarge, E. Gmelin, G.W.H. Höhne, H.K. Cammenga, W. Hemminger and W. Eysel, *Thermochim. Acta*, 247 (1994) 129–168.
- [19] G.W.H. Höhne, W. Dollhopf, K. Blankenhorn and P.U. Mayr, *Thermochim. Acta*, 273 (1996) 17–24.
- [20] B. Wunderlich, M. Möller, J. Grebowicz and H. Baur, *Conformational Motion and Disorder in Low and High Molecular Mass Crystals*, 87. Springer-Verlag, Berlin, Heidelberg, New York, London, Paris, 1988.
- [21] P.J. Holdsworth and A. Keller, *J. Macromol. Sci. Phys. Part B*, 1(3) (1967) 595–604.
- [22] G.W.H. Höhne, W. Hemminger and H.J. Flammersheim, *Differential Scanning Calorimetry*, Springer, Berlin, Heidelberg, New York, 1996.
- [23] P.U. Mayr, unpublished results (1996).
- [24] K.-H. Illers, *Eur. Polym. J.*, 40 (1974) 911.
- [25] G.W.H. Höhne, unpublished results (1996).